The Trajectories of Dropsondes in Simulated Thunderstorm Circulations

CARL E. HANE[1]

National Center for Atmospheric Research,[2] Boulder, Colo. 80303

(Manuscript received 16 December 1974; in revised form 16 April 1975)

ABSTRACT

The trajectories of hypothetical dropsondes are calculated in thunderstorm circulations and resultant vertical wind speed profiles as a function of height are constructed for each of the sondes. Motion fields are a) calculated by a time-dependent two-dimensional thunderstorm model and b) constructed based upon observed environmental winds. Model-calculated vertical wind speed profiles are compared with observations for the northeastern Colorado storm of 22 July 1972. Agreement is shown between certain basic features; additionally, other calculations point to various potential features of dropsonde trajectories and vertical wind speed profiles. Possible application of similar methods to the hail growth problem is discussed.

1. Introduction

A primary goal of the National Hail Research Experiment (NHRE), being conducted in northeast Colorado, is to gain an understanding of all aspects of cloud dynamics and microphysics within damaging hailstorms. Toward this end, an extensive field operation is underway within NHRE to provide observations within and around hailstorms in this region. A critical part of this understanding is a knowledge of the in-cloud air motions and their relations to air motions in the near-cloud environment. In order to measure these air motions, as a part of NHRE, dropsondes have been released above the tops of storms and allowed to fall to the ground. These dropsondes are capable of measuring both vertical and horizontal air motions of the scale and intensity of the cloud circulation. This dropsonde system was developed at the National Center for Atmospheric Research (NCAR) and its engineering and operation have been described in great detail by Bushnell and Glover (1974).

The results of the dropsonde observations are quite often difficult to interpret for several reasons. For one, in some cases only vertical wind speeds as a function of height are determined, with no knowledge of horizontal winds. This occurs when the sondes are dropped too far from the tracking stations for their transmitted signals to be received in a form which is interpretable. A knowledge of the vertical position only does not allow for even a two-dimensional mapping of storm motion. Secondly, it is not always clear where the sondes are measuring air motions in relation to location of the intense portion of the storm's circulation. The purpose of the work described here is to attempt to aid in interpreting the observations by calculating trajectories of such dropsondes in two-dimensional thunderstorm circulations. These circulations are either 1) calculated or 2) geometrically constructed, based upon measured environmental horizontal winds in either case. Although the structure of natural storms is three-dimensional in most cases, it is hoped that the two-dimensional flows will possess sufficient realism in basic structure to obtain some insights into the interpretation of dropsonde measurements obtained in nature. Two-dimensional air motion fields are used rather than three-dimensional fields because of the current availability of two-dimensional convective storm models.

2. Factors affecting dropsonde trajectories

In order to calculate trajectories, it is necessary to know the fall speed of the instrument as a function of height, since over the high plains the instrument falls through air whose density varies from approximately 0.25 to 1.0 kg/m^3. Measurements obtained from test drops of the instruments in the atmosphere are used in this paper to specify terminal fall speed. These test drops were done in northeast Colorado in April 1972 (Bushnell and Glover, 1974) under synoptic conditions which favored little or no vertical air motions. If one plots the fall speed versus height for each of the ten instruments which were dropped, the result is approximately a straight line for each instrument. However,

[1] Present affiliation: Atmospheric Sciences Department, Pacific Northwest Laboratories, Battelle Memorial Institute, Richland, Wash. 99352.

[2] This research was performed as part of the National Hail Research Experiment, managed by the National Center for Atmospheric Research and sponsored by the Weather Modification Program, Research Applications Directorate, National Science Foundation.

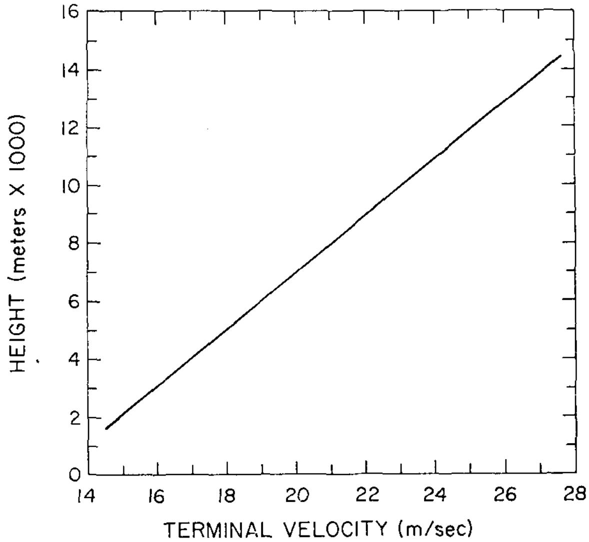

FIG. 1. Dropsonde terminal fall speed as a function of height (MSL) based upon test drops in the atmosphere.

a different straight line is obtained for each instrument, resulting from slight differences among the instruments. At a given height, differences in fall speed between instruments vary from a few tenths to a maximum of about 1 m/s. A median profile has been selected from these ten profiles and has been approximated by a straight line (Fig. 1). The observations obtained from the test drops extended from about 2.5 to 8.5 km (MSL); the straight line in Fig. 1 has been extrapolated downward to 1.6 km (ground elevation) and upward to 14.4 km. Possible effects of icing in changing the effective shape and surface area of the sonde are not considered in the calculations which follow. Changes in terminal fall speed resulting from icing are expected to be small compared to the changes produced by variations in air density, and the uncertainties in the structure of the motion field are too large to warrant consideration of this factor.

In addition to knowing the fall speed of the sonde it is necessary to know how it responds to changes in horizontal air motions as it falls through regions of vertical shear. It has been determined that the sonde's response is such that it moves very nearly with the horizontal component of the wind under all conditions except the most extreme turbulence. Therefore, in the calculations which follow, it is assumed that the horizontal component of the sonde's motion is identical to the horizontal motion of the air around it.

The remaining factor that must be known in order to calculate dropsonde trajectories is the motion of the air itself. This has been approached in two ways here: 1) through calculation of the thunderstorm circulation by a numerical model and 2) through specification of the storm circulation based upon purely geometric considerations and a knowledge of the environmental flow. The first method is somewhat more appealing in that it is objective, but the second method allows for changes to be made easily in the geometry of the updraft and downdraft, and for the testing of the effects of these changes upon dropsonde trajectories.

3. Storm of 22 July 1972

A particular storm was selected for study for which dropsonde data as well as many other types of observations are available. This storm occurred on 22 July 1972 over the NHRE field area in northeastern Colorado. It has been described in great detail elsewhere by Foote and Fankhauser (1973), Bushnell (1973), Eccles (1973), Musil *et al.* (1973), and others. Figure 2 shows soundings taken at Grover, Colo., and Sterling, Colo., at a time when the storm was in one of its most intense stages. The Grover sounding represents conditions in the near-environment west of the storm and the Sterling sounding conditions east of the storm. Two things are noteworthy in Fig. 2: 1) the lower levels are quite dry with dew points 10°C or lower; 2) there is a pronounced stable layer near 300 mb (between 9 and 10 km). The soundings were taken at a time when the storm was roughly halfway between the two stations which are separated by a distance of about 90 km. The dimensions of the storm at this time were roughly 5 to 15 km in the east-west direction and 40 to 50 km in the north-south direction.

The temperature and moisture profiles at Sterling (east of and ahead of the storm) were used as environmental conditions for the model calculations. The temperature field for the model calculations is horizontally

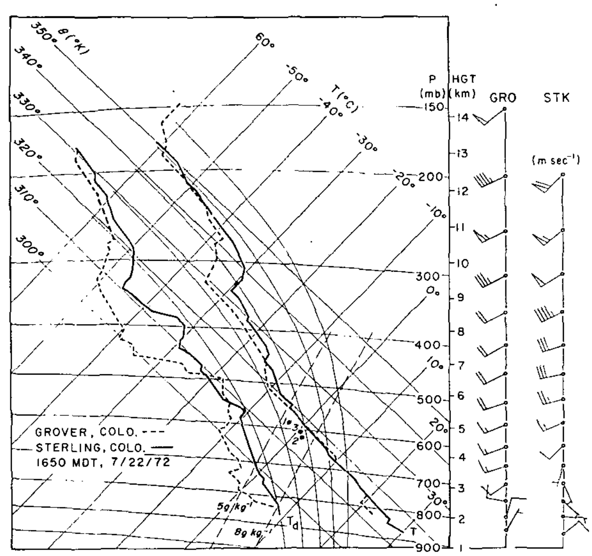

FIG. 2. Vertical profiles of temperature and dew point at Grover and Sterling, Colo., at 1550 MST 22 July 1972. Numbered dots represent condensation temperature and pressure based upon the measurements of various aircraft flying in the inflow region.

homogeneous initially, as is the moisture field except for a perturbation in the lower levels, inserted to hasten the onset of condensation.

The wind field used for the model calculations is based upon the wind soundings at Grover and Sterling shown along the right edge of Fig. 2. The storm motion at this time has been calculated by Foote and Fankhauser (1973) to be approximately 14 m/s from 275°. The plane of integration for the two-dimensional x-z model was chosen to lie in this direction, and the observed winds from Grover and Sterling were projected into it, the component of the wind perpendicular to the direction of storm motion not being taken into account. The Grover wind profile is used to specify the air motion near the left boundary (upshear) and the Sterling sounding, near the right boundary (downshear). This results in a convergent (speed) region near the ground and a divergent region in middle levels (Fig. 3), and therefore upward motion between. This upward motion is specified to be contained within an 8 km wide region initially (total horizontal grid width is 44.4 km) and specified to have a sinusoidal distribution in that region. This results in a region of upward motion 8 km wide and approximately 8 km deep with maximum of a few meters per second near 5 km. This procedure also results in a region of weak downward motion above 8 km which is maximized near 10 km. This is consistent with the location of the previously mentioned inversion, since downward motion should produce warming through adiabatic heating relative to other air which is not moving downward. It should be noted, however, that divergence in the wind component perpendicular to this plane is not taken into account, so that the mesoscale structure to which allusion has been made above is somwhat speculative. The slight alteration of the Grover wind sounding above 10 km is necessary in order that there be no vertical motion through the top boundary of the grid (at 14.4 km). The adjustment is made at the top (see dash-dotted line in upper part of Fig. 3) where wind speed and direction errors are likely to be largest.

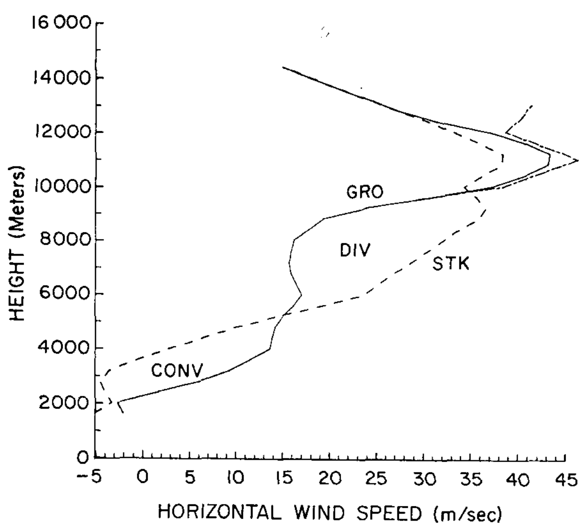

FIG. 3. Component of wind speed in the plane of storm motion as a function of height at Grover and Sterling, Colo., on 22 July 1972, 1650 MST.

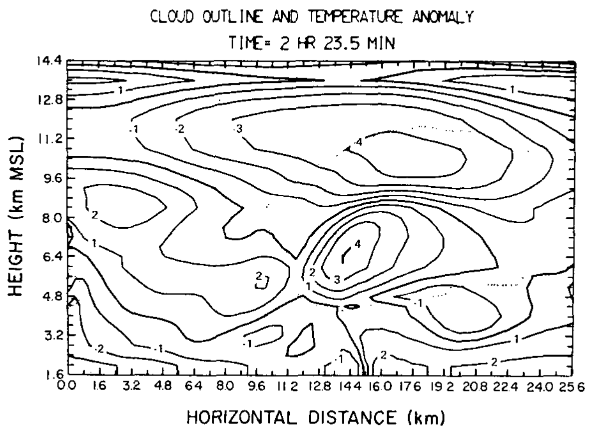

FIG. 4. Cloud outline (dotted) and temperature anomaly (solid) in the model storm of 22 July 1972 at $2^h23.5^m$ model time.

4. The model

The model is exactly the same as described in an earlier paper (Hane, 1973). Only the initial and environmental conditions have been changed to conform to the situation of 22 July 1972. The two-dimensional time-dependent model calculates the horizontal and vertical components of air motion, the temperature, and the water vapor, cloudwater, and rainwater mixing ratios. Included are: 1) the condensation and evaporation processes and their associated temperature changes, 2) liquid water "in bulk" assuming a Marshall-Palmer (1948) distribution of drop sizes, 3) the fall of rain including variable terminal fallspeeds, and 4) turbulent mixing between cloud and environment by scales of motion not resolvable by the 400 m grid. The ice phase is not taken into account. The microphysical treatment of cloud and rain is based upon the formulations of Kessler (1969).

5. Dropsonde trajectories for the 22 July model storm

In presenting the results of model calculations for the 22 July situation, it should be noted that the model results exhibit an oscillatory evolution rather than reaching a quasi-steady state. The intensity of successive peaks in the convective circulation increases with time up to about 2 h model time, then a leveling of successive peaks occurs. These peaks in intensity are separated by approximately 30 minutes. Figure 4 shows the temperature anomaly pattern and cloud outline

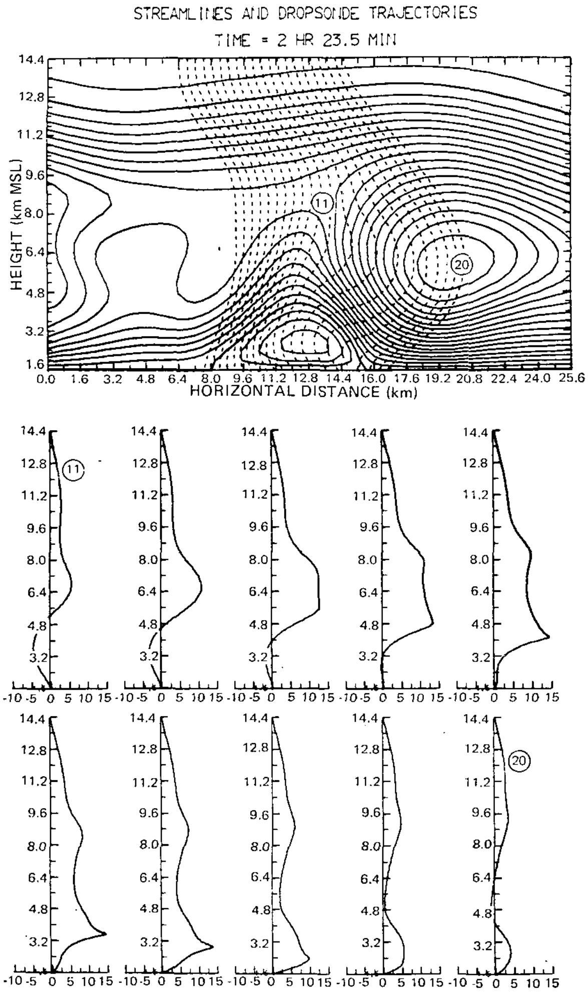

FIG. 5. Upper: Streamfunction (contour interval is 2000 kg m^{-1} s^{-1}) of the relative motion field (solid) and dropsonde trajectories (dashed) in the 22 July 1972 model storm. Lower: Vertical wind speed as a function of height along ten dropsonde trajectories (trajectories 11–20 counting from left).

over a portion of the two-dimensional grid during one of these peaks in intensity (at 2 h 23.5 min following initiation). The cloud base at this time is at about 4.4 km (2.8 km above ground) and the top at 11.6 km. The top half of the cloud is cold and the lower half warm. The cold anomaly in upper levels results from: 1) the dry adiabatic cooling occurring at that level in rising air prior to condensation; 2) the presence of the environmental stable layer between 9 and 10 km. There is a region of warming outside the cloud in mid-levels due to dry adiabatic descent. The air just below cloud base is anomalously cool due to dry-adiabatic cooling in rising air below the condensation level. It may be noted by reference to Fig. 2 that the temperature at cloud base as inferred from aircraft observations (dots in figure) is also anomalously cool. There is a cool axis along the left edge of the cloud and below due to evaporation of rain and a weak micro-cold front at the ground about 15 km from the left boundary. The lack of intense cooling in the rain area is due to the fact that rain has not been falling there for very long. The amount of rain at the ground is much less in the model than was observed in the actual storm. A possible reason for this is the inappropriateness of the Marshall-Palmer drop distribution to the Colorado storms.

Figure 5 shows the relative motion field (relative streamfunction) and dropsonde trajectories at the same time as was shown in Fig. 4. Also shown is the vertical air motion as a function of height along ten of the trajectories (trajectories 11–20, counting from left to right). The maximum vertical velocity in the model updraft at this time is approximately 17 m/s. Also apparent in this figure is the large horizontal variability of the vertical wind speed along the dropsonde trajectories. The form of the profile is quite sensitive to where the sonde enters the cloud. Another very significant feature is the double-maxima shape in certain profiles resulting from the action of the strong shear upon the sonde trajectories. The sonde may be blown through the upper part of the updraft as it falls and be located ahead of the storm for several minutes prior to reentry into the lower portion of the updraft.

Figure 6 shows the vertical wind speed as a function of height as measured by the dropsondes released into the actual storm on 22 July 1972. It is quite important here to point out various reasons why these two sets of profiles should *not* agree. First, the model is two-dimensional, whereas the storm is isolated and there-

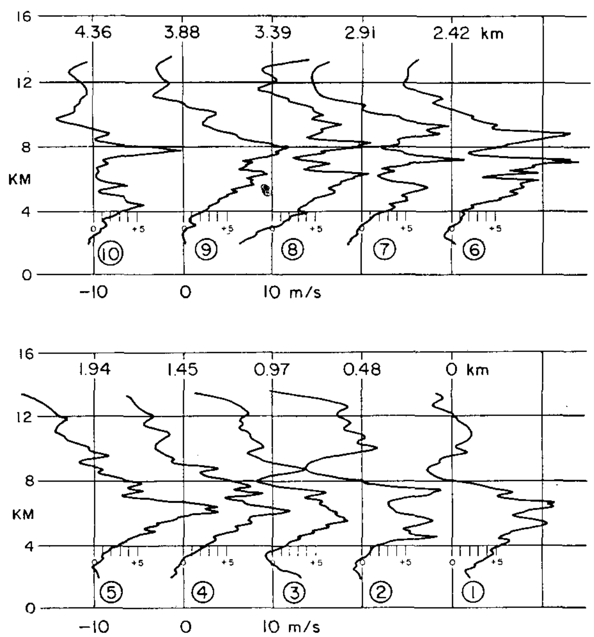

FIG. 6. Vertical wind speed as a function of height along the trajectories of ten dropsondes released into the actual storm of 22 July 1972. Upshear toward upper left and downshear toward lower right (after Bushnell, 1973, but order of presentation reversed).

fore affected by variations in the third dimension. Second, small features of a scale less than approximately 1 km are not resolved by the model. Third, the airplane had a heading of 342° when the drop was made; this is about 70° different from the storm motion vector. Fourth, the updraft air in the actual storm contained air from diverse sources in the remote environment due to the veering of the wind in the subcloud layer in combination with the variable equivalent potential temperature in that layer. The model, on the other hand, is based upon the Sterling sounding alone.

Certain comparisons may be made between calculated and observed, keeping in mind, however, the above four factors. 1) If the short wavelength oscillations are filtered out in the observed profiles, it is seen that the variations are somewhat less than differences between profiles in the model results. This could be a consequence of the plane of the drop cutting across the direction of motion of the storm. 2) Low-level maxima in updraft speed are absent for the most part in the observations; maxima tend to occur at 6–8.5 km MSL in the observations and 4–8 km in the model. This could, again, be a consequence of the aircraft heading and location which did not allow for the possibility of sampling the updraft near the ground further to the east. 3) Certain profiles (e.g., the two in lower right of Fig. 6) suggest that the sondes may have passed in a down-shear direction through the updraft into downward moving air and were then carried by differing horizontal motions at lower levels into the updraft again.

6. Dropsonde sampling as affected by updraft slope

Motion fields which are constructed rather than calculated are advantageous in that changes in basic structure may be prescribed rather simply and the consequent effects upon hypothetical sonde trajectories noted. It may be argued that flow fields constructed upon purely geometric considerations may not represent possible solutions in the real atmosphere, given a set of physical laws and environmental conditions. However, it may also be argued that knowledge may be gained by observing the effects of gross changes in structure even if the individual structures do not correspond perfectly to those possible in nature.

The basic procedure employed here is quite simple, and can best be understood by reference to Figs. 7 and 8. The environmental winds on the left and right of the disturbance are identical to those used in the mcdel calculation of the 22 July 1972 storm circulation. However, in this case, from one calculation of dropsonde trajectories to another, the updraft slope is changed (the slope being defined in terms of the deviation from the vertical of the axis of maximum upward motion). The upward motion occupies a parallelogram-shaped region whose minor angles are equal to the arc cotangent of the updraft slope. The region of downward motion is triangular-shaped and located in the lower levels

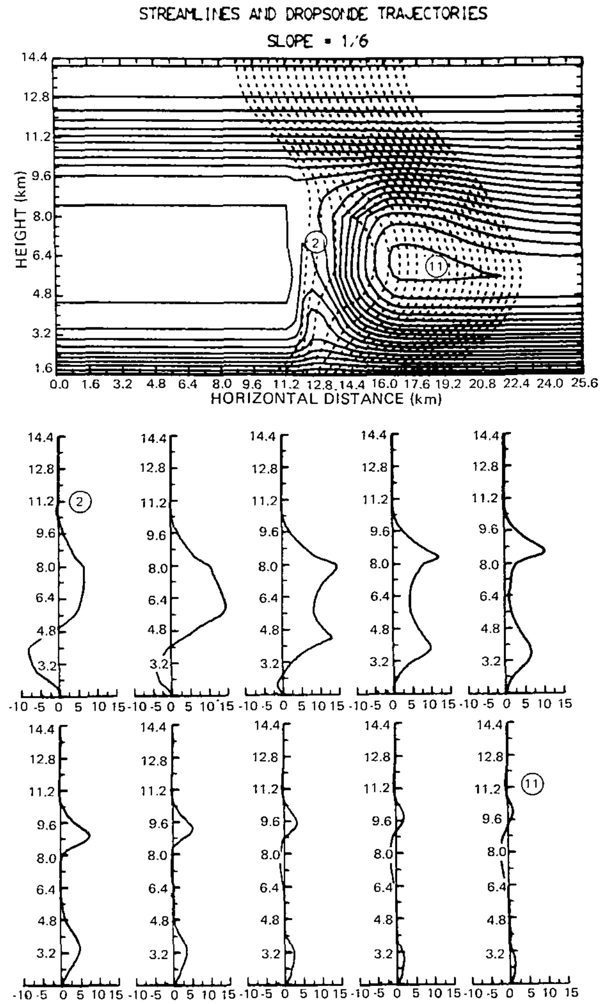

FIG. 7. Same as Fig. 5 for a geometrically constructed storm circulation with updraft slope 1:6 from vertical (trajectories 2–11 from left considered in lower portion of figure).

beneath the updraft. There is also some compensatory downward motion in the region to the right of the updraft.

In Fig. 7 the updraft slope is 1:6 as defined by the $\Delta X:\Delta Z$ along the axis of maximum upward motion. In Fig. 8, on the other hand, the slope is 1:1 (larger deviation from a vertical updraft). Five separate updraft slopes were utilized to calculate sonde trajectories; the two shown here are the extrema of the cases. By comparing the two cases shown, it can be seen that the more vertical updraft is less likely to be well sampled. For example, at a height of 6 to 7 km along the updraft axis the separation between trajectories in the 1:6 slope case is a horizontal distance of 1.5–2.0 km, whereas in the 1:1 slope case it is much less. This separation results from the fact that the horizontal divergence in this plane in the upper updraft region affects an adjacent pair of sondes through much of their fall in the 1:6 slope case. In the 1:1 slope case, however, this

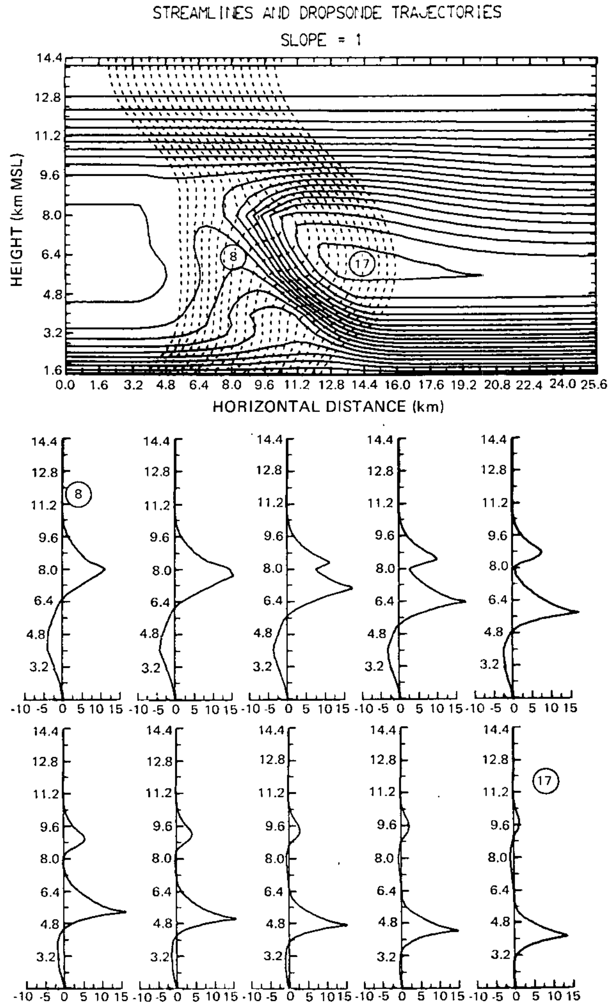

FIG. 8. Same as Fig. 5 for a geometrically constructed storm circulation with updraft slope 1:1 (trajectories 8–17 from left considered in lower portion of figure).

divergence affects a larger number of sondes through a much shorter distance due to their entrance into the updraft at such a large angle.

The profiles of vertical wind speed vs height along the trajectories are quite different in the two cases. In the 1:1 slope case there are a larger number of profiles showing relatively large vertical wind speeds, since more sondes are sampling the strong portion of the updraft. In both cases double maxima in the vertical wind speed versus height are present, as a result of the strong environmental shear; however, a smaller vertical separation in the two maxima exists in the large (1:1) slope case because of the lesser distance traveled to the right (downshear) of the updraft between traverses through the updraft core. In addition, the updraft may not be well sampled both near the ground (note lower section of Fig. 8) and at middle levels by only ten trajectories, simply because of the pronounced updraft slope.

7. Trajectories in an Oklahoma storm

In order to investigate possible trajectories in a more vigorous convective storm, a sounding characteristic of the Oklahoma area was used as input into the same numerical model which was discussed earlier. The basic difference between the soundings in the Oklahoma and Colorado cases is in the low-level moisture values. In terms of mixing ratio the surface moisture in the Oklahoma case is about twice that in the Colorado case. This is a reflection of the difference in elevation between the two locations (surface pressures are approximately 970 and 870 mb) coupled with the characteristic decrease in mixing ratio toward the west in this region of the Plains in summer. The vertical wind shears are comparable in the two cases, slightly weaker in the Oklahoma case. The initial perturbation in this case is a low level convergence zone superimposed upon a

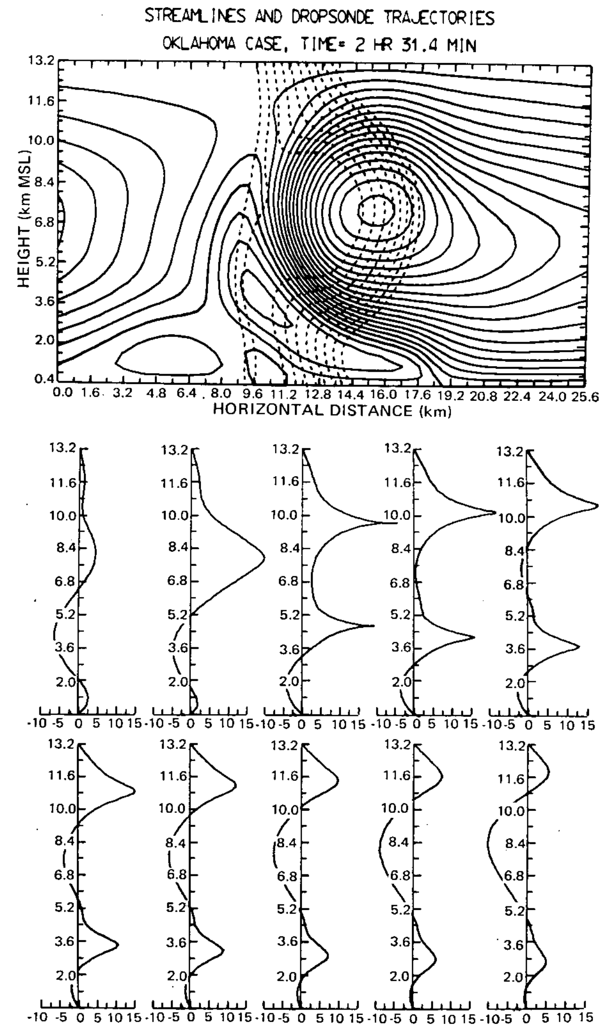

FIG. 9. Same as Fig. 5 but for a model storm existing under environmental conditions characteristic of the Oklahoma area. Hypothetical sondes dropped at intervals of 400 m. Contour interval in this case is increased to 3000 kg m^{-1} s^{-1}.

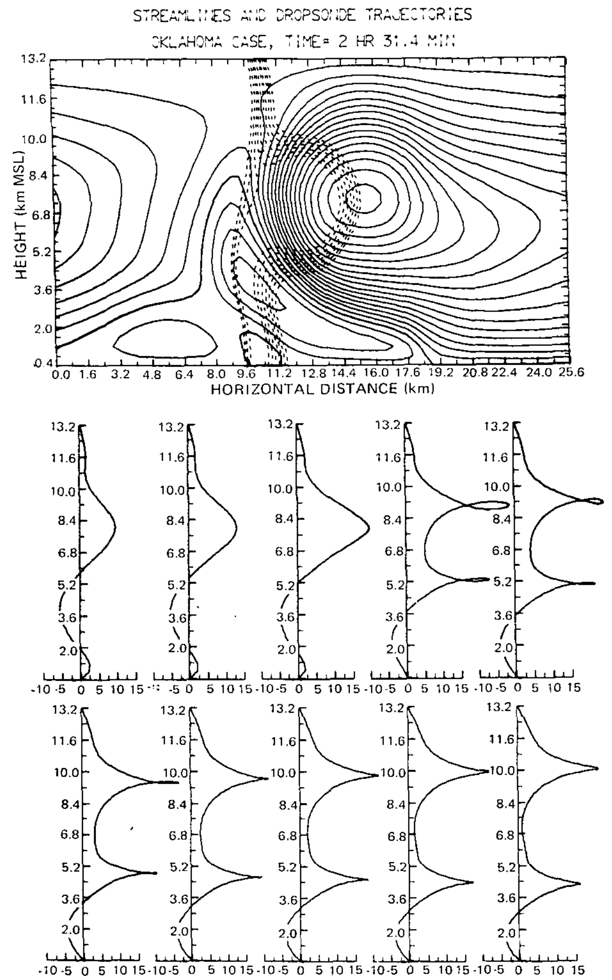

Fig. 10. Same as Fig. 9 but distance between sondes at release point reduced to 100 m.

horizontal moisture gradient of the "dry line" type. The scale and intensity of the dry line have been documented by Fujita (1958), Beebe (1958), McGuire (1962), and National Severe Storms Project staff (1963). The character of the time evolution of the model convection is once again oscillatory with a steady increase in the intensities of successive developments.

Figure 9 shows the relative motion field in the Oklahoma case at approximately 2.5 h following initiation. Superimposed upon this streamfunction field once again are the trajectories of ten dropsondes that fall through this motion field which is assumed to remain steady during the time of the drop. The separation between sondes at the release point at the top of the domain is once again 400 m. The maximum vertical wind speed in the updraft at this time is slightly more than 30 m/s, maximum positive temperature anomaly greater than 10 K, and maximum rainwater mixing ratio about 10 g/kg. A casual examination of Fig. 9 reveals a very extensive area of the updraft which remains unsampled by the sondes. The first and second sondes from the left are diverted to the upshear side of the updraft, whereas the third sonde becomes involved in the updraft and remains at a constant altitude for a short period of time. The eight sondes on the right make two traverses through the updraft as was the case with certain sondes in the preceding sections. The double maxima are clearly shown in the lower part of this figure.

In order to determine the sensitivity of the trajectory to the location of release, the separation between the sondes at the point of release was reduced from 400 m to 100 m. Figure 10 shows the resulting trajectories. As can be seen from the lower sections of Figs. 9 and 10, the second trajectory in Fig. 9 is the same as the third in Fig. 10 and the third in Fig. 9 is the same as the seventh in Fig. 10. Reduction in the separation of the sondes does little to reduce the size of the unsampled region; there is a wide separation between the trajectories of the third and fourth sondes. The fourth, fifth, and sixth sondes are actually carried upward, as revealed by the looping in the vertical wind speed versus height profiles in the lower section of Fig. 10. A further reduction in the separation of the sondes to a distance of 10 m had little influence upon the size of the unsampled region of the updraft (this result not shown).

In Fig. 11 the vertical wind speed along the trajectory of the fourth sonde from the left in Fig. 10 is plotted as a function of time. The two maxima in vertical wind speed are shown to be separated in time by approximately 8 min. The total time of flight is approximately 20 min as compared with about 10 min for the first three sondes on the left. The landing of the third and fourth sondes on the ground is therefore separated considerably both in space and in time.

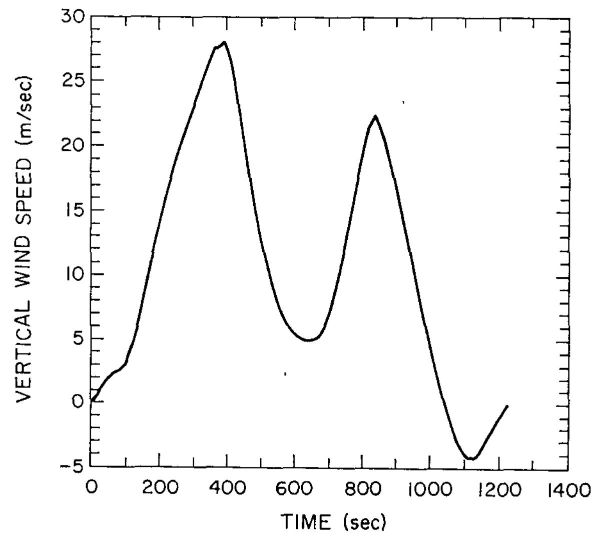

Fig. 11. Vertical wind speed as a function of time after release along the trajectory of the fourth sonde from the left in Fig. 10.

8. Summary and applications to other problems

Certain characteristics of dropsonde trajectories in model storms provide possible clues to the interpretation of vertical wind speed versus height profiles obtained from sondes released in natural situations. The agreement between the calculated and observed profiles is quite encouraging considering the differences (outlined earlier) in various conditions between the two cases. In cases with moderate or strong vertical wind shear, it is quite likely that the profiles should contain at least two maxima or relative maxima in vertical wind speed due to the sonde's passage through the updraft at upper levels and through again in the opposite direction at lower levels. The model calculations indicate a very strong horizontal variation in the vertical separation of these maxima. This horizontal variation is also quite sensitive to updraft slope.

In addition, several difficulties inherent in the use of dropsondes as an observing system are revealed. A sampling problem may arise in cases where the updraft has very little slope from the vertical. This arises due to the trajectories of sondes aligning themselves along lines of maximum horizontal divergence. Likewise, in some cases where the vertical wind speed is very strong, a large region near the updraft maximum may remain unsampled. This results in a dramatic change in the character of adjacent sonde profiles, which may be difficult to interpret from an examination of vertical wind speed versus height profiles alone.

Since model trajectories vary strongly in the horizontal, observed vertical wind speed profiles which show little horizontal variation may be an indication that the airplane heading was nearly normal to the direction of propagation of the storm. This points to a need for pinpointing the location of the drop relative to the storm. Both PPI and RHI radar might then be used more effectively to aid in the interpretation of the vertical wind profiles derived from the sondes.

It is conceivable that the approach outlined here might be used to calculate trajectories of hailstones within model storms, thereby gaining new insights into the relation between a hailstone's history and its resultant structure. The success of this approach would perhaps depend upon whether hailstone structure is more closely related to storm dynamics (e.g., the passage of the stone through the updraft repeatedly) or to microphysical considerations (e.g., the passage of the stone through regions of varying concentrations of supercooled water). The growth of the stone would have to be accounted for (in contrast to the dropsonde) along with changes in terminal fall speed along its trajectory. This could perhaps be done parametrically through consideration of the liquid water and temperature distributions. A more satisfactory attack on the hail growth problem might be made through a detailed microphysical approach such as that of Danielsen *et al.* (1972) with the possible additional consideration of hydrometeor temperatures within the context of a three-dimensional thunderstorm model. Such a detailed treatment is not possible at the present time because of computer size limitations. A parametric approach might in the meantime be employed to provide guidance in the planning of field observational programs and hail suppression experiments.

Acknowledgments. I am most grateful for the encouragement of W. C. Swinbank in the initial stages of this research. Also, I wish to thank C. W. Newton, G. B. Foote, and N. E. LaSeur for their individual comments upon the original manuscript. Discussions with R. H. Bushnell were also very helpful. This research was completed while the author was a summer visitor with the National Hail Research Experiment.

REFERENCES

Beebe, R. G., 1958: An instability line development as observed by the tornado research airplane. *J. Meteor.*, **15**, 278–282.

Bushnell, R. H., 1973: Dropsonde measurements of vertical winds in the Colorado thunderstorm of 22 July 1972. *J. Appl. Meteor.*, **12**, 1371–1374.

——, and V. M. Glover, 1974: A dropsonde for measuring vertical wind in thunderstorms. *Rev. Sci. Instr.*, **45**, 781–788.

Danielsen, E. F., R. Bleck, and D. A. Morris, 1972: Hail growth by stochastic collection in a cumulus model. *J. Atmos. Sci.*, **29**, 135–155.

Eccles, P. J., 1973: Radar echo movement within a hailstorm. *Preprints 8th Severe Local Storms Conf.*, Denver, Colo., Amer. Meteor. Soc., 61–62.

Foote, G. B., and J. C. Fankhauser, 1973: Airflow and moisture budget beneath a northeast Colorado hailstorm. *J. Appl. Meteor.*, **12**, 1330–1353.

Fujita, T. T., 1958: Structure and movement of a dry front. *Bull. Amer. Meteor. Soc.*, **39**, 574–582.

Hane, C. E., 1973: The squall line thunderstorm: Numerical experimentation. *J. Atmos. Sci.*, **30**, 1672–1690.

Kessler, E., 1969: On the distribution and continuity of water substance in atmospheric circulations. *Meteor. Monogr.*, **10**, No. 32, 84 pp.

Marshall, J. S., and W. McK. Palmer, 1948: The distribution of raindrops with size. *J. Meteor.*, **5**, 165–166.

McGuire, E. L., 1962: The vertical structure of three dry lines as revealed by aircraft traverses. *Natl. Severe Storms Proj. Rep. No. 7*, 10 pp.

Musil, D. J., W. R. Sand, and R. A. Schleusener, 1973: Analysis of T-28 aircraft penetrations of a Colorado hailstorm. *J. Appl. Meteor.*, **12**, 1364–1370.

National Severe Storms Project Staff, 1963: Environmental and thunderstorm structures as shown by National Severe Storms Project observations in spring 1960 and 1961. *Mon. Wea. Rev.*, **91**, 271–292.